

GaitEdge: Beyond Plain End-to-end Gait Recognition for Better Practicality

Junaho Liang^{1*}[0000-0001-5612-7631], Chao Fan^{1,4*}[0000-0002-3605-2705], Saihui Hou^{2,4}[0000-0003-4689-2860], Chuanfu Shen^{3,1}[0000-0001-8782-5950], Yongzhen Huang^{2,4}[0000-0003-4389-9805], and Shiqi Yu¹(✉)[0000-0002-5213-5877]

¹ Southern University of Science and Technology
{12132342, 12131100}@mail.sustech.edu.cn

² School of Artificial Intelligence, Beijing Normal University
{housaihui, huangyongzhen}@bnu.edu.cn

³ The University of Hong Kong
noahshen@connect.hku.hk

⁴ Watrix Technology Limited Co. Ltd

Abstract. Gait is one of the most promising biometrics to identify individuals at a long distance. Although most previous methods have focused on recognizing the silhouettes, several end-to-end methods that extract gait features directly from RGB images perform better. However, we argue that these end-to-end methods inevitably suffer from the gait-unrelated noises, *i.e.*, low-level texture and colorful information. Experimentally, we design both the **cross-domain** evaluation and visualization to stand for this view. In this work, we propose a novel end-to-end framework named **GaitEdge** which can effectively block gait-unrelated information and release end-to-end training potential. Specifically, GaitEdge synthesizes the output of the pedestrian segmentation network and then feeds it to the subsequent recognition network, where the synthetic silhouettes consist of trainable edges of bodies and fixed interiors to limit the information that the recognition network receives. Besides, **GaitAlign** for aligning silhouettes is embedded into the GaitEdge without loss of differentiability. Experimental results on CASIA-B and our newly built TTG-200 indicate that GaitEdge significantly outperforms the previous methods and provides a more practical end-to-end paradigm for blocking RGB noises effectively. All the source code will be released.

Keywords: Gait Recognition; End-to-end; Gait Synthesis; Silhouette Alignment; Cross-domain

1 Introduction

In recent years, human identification by walking pattern, *i.e.*, gait, has become a hot research topic. Compared with other biometrics, *e.g.*, face, fingerprint, and iris, human gait can be easily captured at a long distance without the cooperation of subjects, which means gait can be promising for crimes investigation and

* J. Liang and C. Fan are co-first authors.

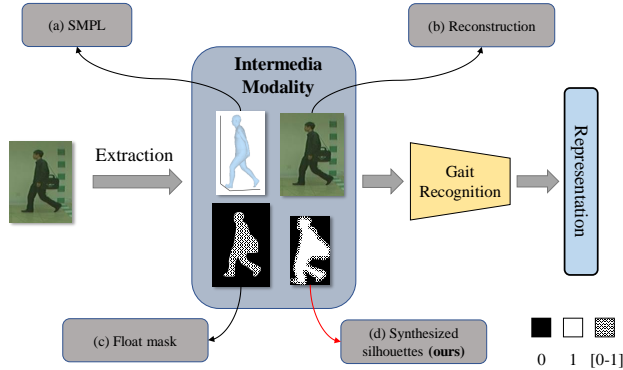


Fig. 1. Three typical end-to-end approaches: (a) model-based end-to-end [14], (b) Zhang’s GaitNet [29], (c) Song’s GaitNet [20] and (d) our **GaitEdge**. *Shaded areas* for the float-point numbers ranging from 0 to 1

suspects tracing under real-world uncontrolled conditions. It is noticed that most of the studies treat gait recognition as a two-step approach, including extracting the intermediate modality, *e.g.*, silhouette mask or skeleton keypoints, from RGB images and putting them into the downstream gait recognition network. However, pieces of research [4,5,7,16] indicate that those multi-step pipelines usually give rise to the weakness in both efficiencies and effectiveness, increasing works are tending to infer the final results directly in end-to-end [29,20,14].

To the best of our knowledge, there are three typical end-to-end gait recognition methods in the recent literature. As illustrated in Figure 1 (a), Li *et al.* [14] utilize a fashion human mesh recovery model [11] to reconstruct the three-dimensional human body and train the recognition network by taking the parameters of the skinned multi-person linear (SMPL) [17] model as inputs. Another typical approach proposed by Zhang *et al.* [29] introduces an autoencoder framework to disentangle the motion-related gait patterns and motion-unrelated appearance features explicitly from the sequential RGB images, as shown in Figure 1 (b). In addition, Song *et al.* propose GaitNet [20], which integrates two tasks, *i.e.*, pedestrian segmentation and gait recognition, as illustrated in Figure 1 (c). It extracts gait features straightly from the intermediate float mask instead of the classical binary silhouettes.

Although achieving higher performance than the two-step methods, we argue that these end-to-end methods cannot ensure that the learned characteristics for human identification only consist of walking patterns and exclude the gait-unrelated features. The reasons are two-fold: (1) Since all the intermediate modalities are float-coding, these relatively soft constraints, *e.g.*, the SMPL reconstruction in [14], posture features disentanglement in [29], and pedestrian segmentation supervision in [20], cannot effectively prevent the network from extracting the gait-unrelated texture and color in its convergence process [13].

(2) All the mentioned end-to-end methods have not conducted persuasive experiments to demonstrate whether the above problem exists.

To alleviate these issues, we notice that gait features are generally more robust for the covariants of camera viewpoints, carrying, and clothing than other gait-unrelated noises, *i.e.*, texture and color, which implies that if these uncorrelated features dominate in the extracted gait representations, the recognition performance will drop a lot when the model is directly exploited in unseen domains (new dataset) [8]. Hence, in this paper, we introduce the **cross-domain** evaluation to expose the side effects of RGB information. More importantly, we propose a concise yet compelling end-to-end framework named **GaitEdge** to deal with this challenging evaluation. As shown in Figure 1 (d), the intermediate modality of GaitEdge is a novel synthetic silhouette, while its edge is composed of the trainable float mask, and other regions are classical binary silhouettes. Two intuitive phenomena inspire this design: First, the RGB-informed noises are mainly distributed in the non-edge regions, *e.g.*, the human body and background. Therefore, treating these regions as binary silhouettes can effectively prevent the leakage of gait-unrelated noises. Second, the edge region plays a vital role in describing the shape of the human body. Hence, making the only edge region trainable is enough to liberate the potential of the end-to-end training strategy. In addition, we observe that the size-normalized alignment [9] is necessary for the silhouette pre-processing to keep the body in aspect ratio. Unfortunately, this operation used to be offline and thus non-differentiable, which means it can not be directly applied to align the synthetic silhouette. To solve this problem, inspired by the RoIAlign [6], we propose **GaitAlign** module to complete the framework of GaitEdge, which can be regarded as a differentiable version of the alignment method proposed by [9].

In summary, we make the following three major contributions: (1) We point out the worry about gait-unrelated noises being mixed into the final gait representations and introduce cross-domain testing to verify the leakage of RGB-informed noises. Besides, due to the lack of a gait dataset providing RGB videos, we collect the *Ten Thousand Gaits* (TTG-200), whose size is approximately equal to the popular CASIA-B [25]. (2) We propose the GaitEdge, a concise yet compelling end-to-end gait recognition framework. Experiments on both CASIA-B and TTG-200 indicate that GaitEdge reaches a new state-of-the-art performance and declares that GaitEdge can effectively prevent irrelevant RGB-informed noises. (3) We propose an introductory module named GaitAlign for the silhouette-based end-to-end gait recognition, and it can be considered a differentiable version of size-normalization [9].

2 Related Work

2.1 Gait Recognition

As a kind of biometrics, gait is defined by early research [23] as the walking pattern that a given person will perform in a fairly repeatable and characteristic way. On the other hand, another similar task, *i.e.*, person re-identification [30],

aims to find a person presented in one camera in another place by another camera. Despite the similarity, they are still fundamentally different: the first task focuses on walking patterns, while the second task uses clothing primarily for identification. Therefore, it is worth emphasizing that we can not let the gait recognition network acquire information other than gait patterns, such as RGB-informed texture and color.

At present, the mainstream visual-based gait recognition methods can be roughly divided into model-based and appearance-based. The former model-based approaches [15,2,14,22] usually extract the underlying structure of the human body first, *e.g.*, 2D or 3D skeleton key-points, and then model the human walking patterns. In general, such methods can better mitigate the effects of clothing and more accurately describe the body's posture. Nonetheless, all of them are difficult to model the human body structure under the practical surveillance scene due to the low quality of the video.

More and more appearance-based gait recognition methods [24,27,4,28,5,7,16] are currently leaving model-based methods behind. Since GaitSet [4] regarded the gait sequence as an unordered set and achieved high accuracy on CASIA-B, this sort of set-based approaches [4,5,7,16] has attracted increasing attention. For example, Fan *et al.* [5] propose a novel focal convolutional layer to learn the local part feature and then utilize Micro-motion Capture Module to model short-range temporal patterns. Besides, Lin *et al.* [16] propose a 3D CNN-based Global and Local Feature Extractor module to attain discriminative global and local representations from gait frames, which outperforms the other methods remarkably.

2.2 End-to-end Learning

End-to-end learning refers to integrating several separate gradient-based deep learning modules in a differentiable manner. This training paradigm has a natural advantage in that the system optimizes components for overall performance rather than optimizing human-selected intermediates [3].

Recently, some excellent research has benefited from the end-to-end learning paradigm. For example, Amodei *et al.* [1] replace entire pipelines of hand-engineered components with neural networks to overcome the diverse variety of speech by end-to-end learning. Another notable work [3] is Nvidia's end-to-end training for autonomous driving systems. It only gives the system the human steering angle as the training signal. Still, the system can automatically learn the internal representation of the necessary processing steps, such as detecting lane lines.

As the end-to-end philosophy becomes increasingly popular, several studies [29,14,20] have applied it to gait recognition. For instance, Zhang *et al.* [29] propose an autoencoder to disentangle the appearance and gait information without the explicit appearance and gait label for supervision. However, this method is hard to ensure that the disentangled information only consists of motion features and gait patterns. Secondly, Li *et al.* [14] use the newly developed 3D human mesh model [17] as an intermediate modality and make the silhouettes generated

by the neural 3D mesh renderer [12] consistent with the silhouette segmented from RGB images. Because the 3D mesh model provides more helpful information than silhouettes, this approach achieves state-of-the-art results. However, using a 3D mesh model requires a higher resolution of an input RGB image, which is not feasible in the real surveillance scenario. Unlike the previous two, Song et al. [20] proposed another type of end-to-end gait recognition framework. It is formed by directly connecting the pedestrian segmentation and gait recognition networks, which is supervised by a joint loss, *i.e.*, segmentation loss and recognition loss. This approach looks relatively more applicable, but it is also likely to result in the gait-unrelated noises leaking into the recognition network due to the absence of explicit restrictions. Under this consideration, Our Gait-Edge mainly poses and addresses two pivotal problems: cross-domain evaluation and silhouette misalignment.

3 Cross Domain Problem

From the previous perspective, we argue that although the existing end-to-end approaches [29,20,14] greatly improve the accuracy, it is natural to suspect that the introduction of RGB information is the cause of the improvement. To verify our conjecture, we introduce two gait recognition paradigms and compare them experimentally.

Firstly, one of the best-performing two-step gait recognition methods, *i.e.*, **GaitGL** [16], is adopted as a baseline. In addition, a simple and straightforward end-to-end model named **GaitGL-E2E** that provides a fair comparison is introduced. As shown in Figure 2 (a) and (b), both methods use the same modules except that GaitGL-E2E replaces binary mask with float-coding silhouettes through a trainable segmentation network, *i.e.*, U-Net [18]. Experimentally, we define the **single-domain** evaluation as training and testing on CASIA-B*⁵ [25]. Correspondingly, the **cross-domain** evaluation is defined as training on another dataset, *i.e.*, TTG-200, similar to CASIA-B* but testing the trained model on CASIA-B*. More implementation details will be elaborated in Section 5.

As shown in the single-domain part of Figure 2 (d), GaitGL-E2E easily outperforms GaitGL because it has more trainable parameters, and more information is contained in the float-point numbers of silhouettes at the same time. However, it is inevitable to doubt that float-point numbers flowing into the recognition network bring in texture and color from RGB images, which makes the recognition network learn gait-unrelated information and leads to the degradation of cross-domain performance. On the other hand, the cross-domain part of Figure 2 (d) shows that GaitGL-E2E does not achieve the same advantages as it does in single-domain and is even much lower than GaitGL (GaitGL: 40.34%, GaitGL-E2E: 27.18%) in the most challenging case, *i.e.*, CL (walking with cloth change). This phenomenon indicates that the end-to-end model may learn low-level cloth information rather than gait pattern.

⁵ We re-annotate CASIA-B and denote the newly processed one as CASIA-B*.

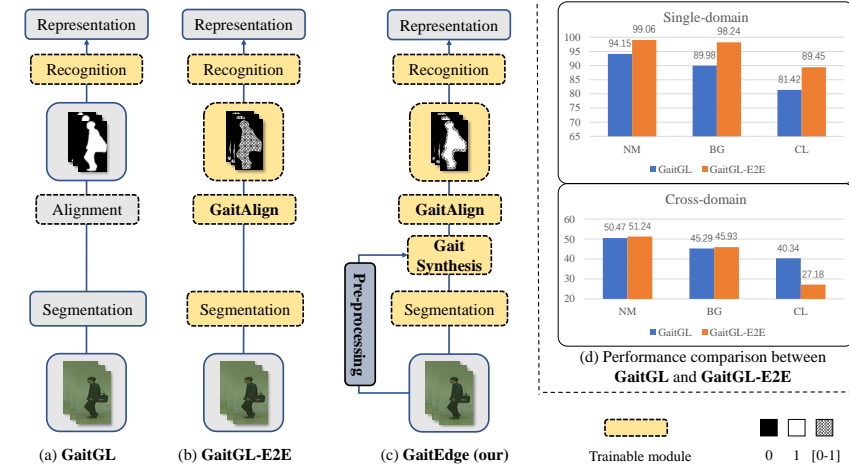


Fig. 2. (a), (b) and (c) are three different frameworks. (d) The rank-1 accuracy (%) on CASIA-B* excluding identical-view cases. *NM* for normal walking, *BG* for walking with bags, and *CL* for walking with cloth change

The above two experiments demonstrate that GaitGL-E2E does absorb RGB noises so that it is no longer reliable for gait recognition with practical cross-domain requirements. Therefore, we propose a novel framework GaitEdge composed of our carefully designed Gait Synthesis module and differentiable GaitAlign module, as shown in Figure 2 (c). The most significant difference between GaitEdge and GaitGL-E2E is that we control the transmission of RGB information through manual silhouettes synthesis.

4 Our Framework

4.1 Gait Synthesis

We generally believe that the edge (the boundary of the silhouette) contains the most discriminative information in silhouette images. The interior of a silhouette can be regarded as low-frequency content with less information, whereas the information will be too sparse to train the recognition network if we get rid of the interior. Therefore, the designed module, named **Gait Synthesis**, focuses on combining trainable edges with fixed interiors through mask operation. It only trains the edge part of the silhouette image, and the region other than edges are extracted from the frozen segmentation network. As shown in Figure 3, to clarify how our framework works, we use yellow for the trainable module and illustrate the flow of gradient transfer, in which the dotted orange line represents the backward propagation, and the solid blue line represents the forward propagation. The masks of edge and interior are denoted as M_e and M_i . The output probability of the segmentation network is denoted as P . Then, the output of

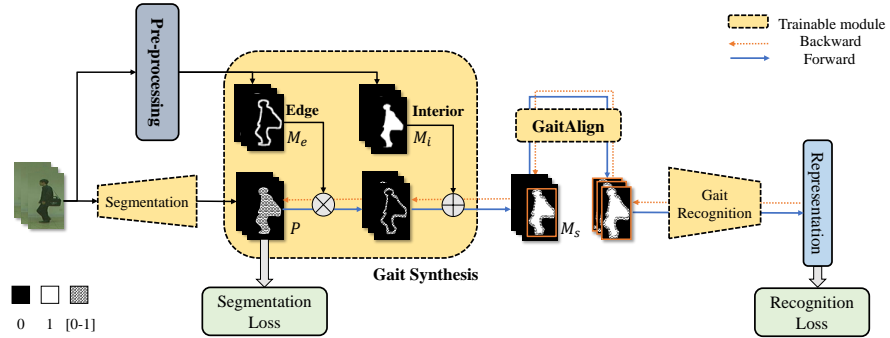


Fig. 3. Illustration of GaitEdge, \oplus for *add element-wise*, \otimes for *multiply element-wise*, and *shaded areas* for float-point numbers ranging from 0 to 1. More details about **Pre-processing** module can be found in Figure 4.

Gait Synthesis denoted M_s can be obtained by several element-wise operations:

$$M_s = M_e \times P + M_i \quad (1)$$

As shown in Equation 1, we explicitly multiply P by M_e and then add it to M_i , which blocks most information, including the gait-related and gait-unrelated. However, we can still fine-tune the edges of the silhouettes, making it automatically optimized for recognition.

Pre-processing. We design an untrainable pre-processing operation to get M_e and M_i , shown in Figure 4. Specifically, we divide it to three steps. First, we segment the input RGB image with the trained segmentation model to obtain the silhouette M . Then, in the second step, we use the classic morphological algorithms to get the dilation and erosion silhouettes(M_i) with a 3×3 flat structuring element. Finally, we get M_e by element-wise exclusive or \vee . Formally:

$$\begin{aligned} M_i &= \text{erode}(M) \\ M_e &= M_i \vee \text{dilate}(M) \end{aligned} \quad (2)$$

Overall, *Gait Synthesis* takes the most intuitive approach by limiting the adjustable region to retain the most valuable silhouette features while eliminate

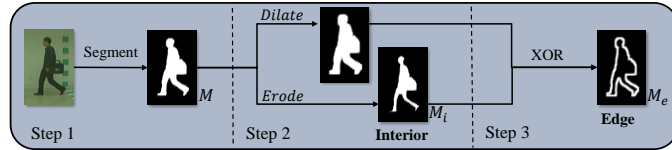


Fig. 4. The **Pre-processing** module in GaitEdge, and it can extract edge regions of silhouettes.

Algorithm 1 Pseudocode of GaitAlign in a PyTorch-like style.

```

# s_in : silhouettes from segmentation output, (nx1hxw)
# size : the target size, (H,W)
# r : aspect ratio of human body, (n)
# s_out : aligned silhouettes, (nx1HxW)

# pad along the x axis so as not to exceed the boundary
s_in = ZeroPad2d((w // 2, w // 2), 0, 0) # (nx1hx2w)
binary_mask = round(s_in) # binary silhouette

# compute the coordinates and restore the aspect ratio r
left, top, right, bottom = bbox(binary_mask, r, size)

# get the new silhouettes by differentiable roi_align
s_out = roi_align(s_in, (left, top, right, bottom), size)

```

bbox: Get the four regularly locations of bounding box keeping aspect ratio. We hide this tedious engineering trick, and the source code will be released.

roi_align: Crop and resize the interested region without the loss of spatial alignment.

most of low-level RGB-informed noises. It is worth mentioning that, *Gait Synthesis* can be detachably integrated into previous silhouette-based end-to-end methods due to the simplicity of the design.

4.2 Gait Alignment Module

Alignment is very crucial for all silhouette-based gait recognition methods. Since the size-normalization of the silhouette has been used for the first time on the OU-ISIR Gait Database [9], almost all silhouette-based methods pre-process the silhouette input via size-normalization, which removes the noise and benefit the recognition. However, the previous end-to-end approach, *i.e.*, GaitNet [20], feeds the segmented silhouette into the recognition network directly, which hardly handles the situation mentioned above. Therefore, we propose a differentiable Gait Alignment Module called *GaitAlign* to make the body be the center of the image and fill the entire image vertically.

We first review the size-normalization [9] procedure because GaitAlign can be regarded as a differentiable version. In size-normalization, by figuring out the top, bottom, and horizontal center of the body, we can scale the body to the target height in aspect ratio and then pad the x-axis with zeros to reach the target width. In our case, pseudo-code in Algorithm 1 depicts the procedure of GaitAlign. We first need to pad the left and right sides with half the width of zeros, which ensures that crop operation will not exceed the boundary. According to the aspect ratio and the target size, then we compute the exact values of four regularly sampled locations. Finally, RoIAlign [6] is applied to the locations given by the previous step. As a result, we get the standard-size, image-filled silhouettes, and its aspect ratio remains the same (refer to the output of GaitAlign in Figure 3). Another noteworthy point is that the GaitAlign module is still **differentiable**, making our end-to-end training feasible.



Fig. 5. Examples of CASIA-B and TTG-200. The left (CASIA-B) consists of six views of one sequence. The right (TTG-200) consists of six subjects with different views

5 Experiment

5.1 Settings

Datasets. There are a few available datasets for gait recognition, *e.g.*, CASIA-B [25], OUMVLP [21], Outdoor-Gait [20], FVG [29], GREW [31], and so on. However, not all of them are useful for the end-to-end based gait recognition methods. For example, the proposed work cannot apply two of the worldwide largest gait datasets, OUMVLP [21] and GREW [31], because both of them provide no RGB videos. In short, our ideal gait dataset owns several vital attributes: RGB videos available, rich camera viewpoints, and multiple walking conditions.

CASIA-B [25] seems to be a good choice. Nevertheless, there still needs another similar dataset to fit our cross-domain settings. Consequently, we collect a private dataset named *Ten Thousand Gaits 200 (TTG-200)* and show its statistics in Table 1.

CASIA-B. There are 124 subjects walking indoor in CASIA-B. It is probably the most popular dataset that consists of 11 views ($[0^\circ-180^\circ]$) and three walking conditions, *i.e.*, normal walking (NM#01-06), walking with bags (BG#01-02), and walking with cloth change (CL#01-02). We strictly follow previous studies, which group the first 74 subjects into the training set and others into the test set. Furthermore, for the test stage, the first 4 sequences (NM#01-04) are regarded as the gallery set, while the left 6 sequences are grouped into 3 probe subsets, *i.e.*, NM#05-06, BG#01-02, CL#01-02. Besides, since the silhouettes of CASIA-B were obtained by the outdated background subtraction, there exists much noise

Table 1. The statistics of existing gait datasets and our collected TTG-200

Dataset	Subjects	Environment	Format	Variations	#Sequences
CASIA-B	124	Indoor	RGB	11 views, carrying, clothing	13636
OUMVLP	10307	Indoor	Silhouette	14 views	267388
FVG	226	Outdoor	RGB	3 frontal views, walking speed, carrying, clothing, background	2856
Outdoor-Gait	138	Outdoor	RGB	carrying, clothing	4964
GREW	26345	Outdoor	Silhouette	multiple camera	128671
TTG-200 (our)	200	Outdoor	RGB	12 views, carrying, clothing, talking on the phone, background	14198

caused by the background and clothes of subjects. Hence, we re-annotate the silhouettes of CASIA-B and denote it as *CASIA-B**. All our experiments are conducted on this newly annotated one.

TTG-200. This dataset contains 200 subjects walking in the wild, and each subject is required to walk under 6 various conditions, *i.e.*, carrying, clothing, taking on the phone, and so on. For each walking process, the subject will be captured by 12 cameras located around the different viewpoints (unlabelled), which means each subject ideally owns $6 \times 12 = 72$ gait sequences. In the following experiments, we take the first 120 subjects for training and the last 80 subjects for the test. In addition, the first sequence (#1) is regarded as gallery set, and the left 5 sequences (#2-6) are regarded as probe set.

As shown in Figure 5, compared with CASIA-B, TTG-200 has three main differences: (1) The backgrounds of TTG-200 are more complex and diverse (collected in multiple different outdoor scenes); (2) The data of TTG-200 are mostly aerial view, while data of CASIA-B are mostly horizontal view; (3) TTG-200 has better image quality. Therefore, we can treat these two datasets as different domains.

Implementation Details

Data Pre-processing. We first employ ByteTrack [26] to detect and track pedestrians from the raw RGB videos for both CASIA-B [25] and TTG-200, and then conduct the human segmentation and silhouette alignment [9] to extract the gait sequences. The obtained silhouettes are resized to 64×44 and can be taken as the input of these two-stage gait recognition methods or be the ground-truth for the pedestrian segmentation network in these end-to-end based approaches.

Pedestrian Segmentation. We use the popular U-Net [18] as our segmentation network that is supervised by Binary Cross-Entropy [10] loss L_{seg} . We set the input size as $128 \times 128 \times 3$ and the channels of U-Net as $\{3, 16, 32, 64, 128, 64, 32, 16, 1\}$ and train it via SGD [19] (batch size=960, momentum=0.9, initial learning rate=0.1, weight decay= 5×10^{-4}). For each dataset, we train the network with learning rate scaled to 1/10 two times for every 10000 iterations until convergence.

Gait Recognition. We use the latest GaitGL [16] as our recognition network and strictly follow the original paper’s settings.

Joint Training Details. In this step, the training data sampler and batch size are similar to the gait recognition network. We jointly fine-tune the segmentation and recognition networks with the joint loss $L_{joint} = \lambda L_{seg} + L_{rec}$,

where L_{rec} denotes the loss of recognition network. The λ represents the loss weight of segmentation network and is set to 10. Besides, to make the joint training process converge faster, we use the trained segmentation and recognition

Table 2. The rank-1 accuracy (%) on CASIA-B* and TTG-200. The identical-view cases in CASIA-B* are excluded. The **bold** and **(bold)** numbers for the two highest accuracies of single-domain and that of cross-domain, respectively

Training Set	Method	Test Set				TTG-200	
		CASIA-B*					
		NM	BG	CL	Mean		
CASIA-B*	Two-step	GaitSet [4]	92.30	86.10	73.36	83.92	40.26
		GaitPart [5]	93.14	85.99	75.05	84.72	42.23
		GaitGL [16]	94.15	89.98	81.42	88.52	(48.74)
	End2end	GaitGL-E2E	99.06	98.24	89.45	95.58	37.18
		GaitEdge	97.94	96.06	86.36	93.45	(49.12)
TTG-200	Two-step	GaitSet [4]	41.32	35.15	21.59	32.69	77.62
		GaitPart [5]	45.21	38.75	25.92	36.62	80.24
		GaitGL [16]	50.47	45.29	40.34	(45.37)	80.46
	End2end	GaitGL-E2E	51.24	45.93	27.18	41.45	90.37
		GaitEdge	54.76	49.85	38.16	(47.59)	88.66

networks parameters to initialize the end-to-end model, and accordingly, their initial learning rate is set to 10^{-3} and 10^{-4} , respectively. Moreover, we fix the first half of the segmentation network, *i.e.*, U-Net, to keep the segmentation result in human shape. We jointly train the end-to-end network for a total of 20,000 iterations and reduce the learning rate by 1/10 at the 10,000th iteration.

5.2 Performance Comparison

To demonstrate the reliable cross-domain capability of GaitEdge, we conduct the single-domain and cross-domain evaluations on CASIA-B* and TTG-200, as shown in Table 2.

The diagonal of Table 2 shows the single-domain performance comparisons, where these methods are trained and evaluated in the identical dataset. Opposite, the anti-diagonal shows the cross-domain performance comparisons, where these methods are trained and evaluated in the different datasets.

Single-domain Evaluation. From the diagonal results in Table 2, we observe that the performances of traditional two-step gait recognition methods are far inferior to that of two end-to-end ones. For example, GaitGL-E2E exceeds GaitSet [4] by 11.66% for CASIA-B* and 12.75% for TTG-200, respectively. On the other hand, the accuracy of our proposed GaitEdge is slightly lower than that of GaitGL-E2E, *i.e.*, -2.13% for CASIA-B* and -1.71% for TTG-200. However, we argue that GaitGL-E2E owns the higher risk of overfitting in the gait-unrelated noises since it directly takes the float mask generated by the segmentation network as the input of the recognition network. Hence, we further conduct the cross-domain evaluation to stand for this point of view experimentally.

Cross-domain Evaluation. If some irrelevant noises dominate the gait representations used for human identification, *i.e.*, texture and color, the recognition

Table 3. The rank-1 accuracy (%) on CASIA-B* across different views excluding the identical-view cases. For evaluation, the first 4 sequences (NM#01-04) are regarded as the gallery set, while the left 6 sequences are grouped into 3 probe subsets, *i.e.*, NM#05-06, BG#01-02, CL#01-02. The original paper of Song GaitNet does not mention the results of BG and CL

Probe	Method	Probe View												Mean
		0°	18°	36°	54°	72°	90°	108°	126°	144°	162°	180°		
NM	Song GaitNet [20]	75.60	91.30	91.20	92.90	92.50	91.00	91.80	93.80	92.90	94.10	81.90	89.90	
	Zhang GaitNet [28]	93.10	92.60	90.80	92.40	87.60	95.10	94.20	95.80	92.60	90.40	90.20	92.30	
	HMRGait [14]	96.90	97.10	98.50	98.40	97.70	98.20	97.60	97.60	98.00	98.40	98.60	97.90	
	GaitEdge	97.20	99.10	99.20	98.30	97.30	95.50	97.10	99.40	99.30	98.50	96.40	97.90	
BG	Zhang GaitNet [28]	88.80	88.70	88.70	94.30	85.40	92.70	91.10	92.60	84.90	84.40	86.70	88.90	
	HMRGait [14]	94.80	92.90	93.80	94.50	93.10	92.60	94.00	94.50	89.70	93.60	90.40	93.10	
	GaitEdge	95.30	97.40	98.40	97.60	94.30	90.60	93.10	97.80	99.10	98.00	95.00	96.10	
CL	Zhang GaitNet [28]	50.10	60.70	72.40	72.10	74.60	78.40	70.30	68.20	53.50	44.10	40.80	62.30	
	HMRGait [14]	78.20	81.00	82.10	82.80	80.30	76.90	75.50	77.40	72.30	73.50	74.20	77.60	
	GaitEdge	84.30	92.80	94.30	92.20	84.60	83.00	83.00	87.50	87.40	85.90	75.00	86.40	

accuracy would drop dramatically in the case of cross-domain settings since the extracted features represent the relatively robust gait patterns impotently. The anti-diagonal results in Table 2 shows that all these methods have colossal performance degradation compared to single-domain due to the significant difference between CASIA-B* and TTG-200. We notice that although GaitGL-E2E has the highest accuracy in single-domain, it achieves the poorest performance for crossing the domain from CASIA-B* to TTG-200. In contrast, though lost by just about two points to GaitGL-E2E in single-domain, our GaitEdge reaches the best performances than any other posted methods in cross-domain evaluations. Hence, this cross-domain evaluation not only indicates the robustness of GaitEdge is far superior to that of GaitGL-E2E but also claims the GaitEdge is a practical and advanced framework for the end-to-end gait recognition task.

Comparison with other end-to-end methods. Last but not least, the proposed GaitEdge is compared to three previous end-to-end gait recognition methods across different views on CASIA-B*. Table 3 shows that GaitEdge reaches the highest accuracy on various walking conditions, especially for CL (+20.1% than Zhang GaitNet, +8.8% than HMRGait), which reveals that GaitEdge is remarkably robust to color and texture (cloth change).

5.3 Ablation Study

In this section, we provide the ablation study to show the effectiveness of every innovation in Section 4. The experiment settings refer to Section 5.1.

Impact of Edge. Table 4 shows the impact of body edge size. We extract the edges by several sizes of structuring elements—the larger the structuring element, the larger the edge area. According to the results shown in Table 4, as the size of the structuring element increases, the performance of single-domain



Fig. 6. (a) The original images (top) *vs.* the disturbed images (bottom). We make random pixel offset to the disturbed images, including vertical and horizontal direction. (b) The ablation study for the *GaitAlign* module. The results are reported on CASIA-B* after disturbance

accordingly increases, but the performance of cross-domain almost decreases at the same time. This result claims that the area of the float mask occupying the intermediate synthetic silhouette is negatively associated with the cross-domain performance for GaitEdge. Therefore, we can assert that GaitGL-E2E fails in cross-domain evaluation because it is equivalent to GaitEdge in the case of infinite structural element. Furthermore, those non-edge regions of silhouette, *i.e.*, human body and background, are unsuitable in float-coding for the end-to-end gait recognition framework.

Impact of GaitAlign. Notably, we observe that the result of pedestrian detection (upstream task) in natural scenes, is often much worse than that of the controlled environment, *i.e.*, CASIA-B* and TTG-200. In order to simulate such a complex situation, we first apply object detection on the videos of CASIA-B*

Table 4. The ablation study for the size of structuring element. The larger size for the larger edge region. The **bold** and **(bold)** numbers for the highest accuracy of single-domain and that of cross-domain, respectively

Training Set	Method	Structuring Element	Test Set				TTG-200	
			CASIA-B*					
			NM	BG	CL	Mean		
CASIA-B*	GaitEdge	3 × 3	97.94	96.06	86.36	93.45	-	
		5 × 5	98.88	97.36	88.24	94.83	49.12	
		7 × 7	98.97	97.90	88.36	95.08	(50.98)	
		9 × 9	99.02	98.19	89.05	95.42	49.15	
		GaitGL-E2E	-	99.06	98.24	89.45	95.58	
TTG-200	GaitEdge	3 × 3	54.76	49.85	38.16	(47.59)	88.66	
		5 × 5	49.21	45.22	33.71	42.71	89.62	
		7 × 7	50.26	44.20	32.43	42.29	90.00	
		9 × 9	48.84	41.72	27.66	39.41	90.39	
		GaitGL-E2E	-	51.24	45.93	27.18	41.45	

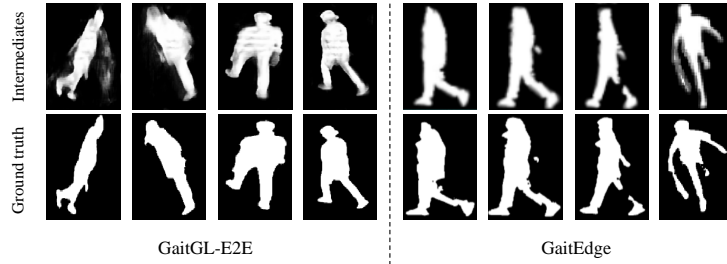


Fig. 7. The comparison between the generated intermediates and ground truth. The first rows are intermediates generated by GaitGL-E2E and GaitEdge, respectively. The second rows are corresponding ground truths

and then perform random pixel offset along with vertical and horizontal coordinates with a probability of 0.5. As shown in Figure 6 (a), the bottom images are disturbed, aiming to simulate the complex situation in natural scenes. Figure 6 (b) shows that alignment improves the average accuracy significantly. In addition, we also notice that the accuracy of normal walking (NM) drops a little, *i.e.*, -0.38%. However, we believe this is because the accuracy of NM has reached a bottleneck.

5.4 Visualization

To better understand the performance degradation of GaitGL-E2E in cross-domain and the effectiveness of GaitEdge, we visualize the intermediates generated by both methods, as shown in Figure 7. The comparison between the intermediates generated by GaitGL-E2E and ground truth shows float-point numbers do introduce some texture and color (black and white stripes on the body) that we want to get rid of. On the right side of Figure 7, our proposed GaitEdge looks to fix some poorly segmented silhouettes, such as filling in the gap in legs, and brings no gait-unrelated information because it only fine-tunes the edges.

6 Conclusion

This paper presents a novel end-to-end gait recognition framework termed GaitEdge that can solve the performance degradation in cross-domain situation. Specifically, we design a Gait Synthesis module to mask the fixed body with tunable edges obtained by morphological operation. Besides, a differentiable alignment module named GaitAlign is proposed to solve the body position jitter caused by the upstream pedestrian detection task. We also conduct extensive and comprehensive experiments on two datasets, including reprocessed CASIA-B* and our newly built TTG-200. Experimental results show that GaitEdge significantly outperforms the previous methods, indicating that GaitEdge is a

more practical end-to-end paradigm that can effectively block RGB noise. Moreover, this work exposes the cross-domain problem that has been neglected by previous studies, which provides a new perspective for future research.

References

1. Amodei, D., Ananthanarayanan, S., Anubhai, R., Bai, J., Battenberg, E., Case, C., Casper, J., Catanzaro, B., Cheng, Q., Chen, G., et al.: Deep speech 2: End-to-end speech recognition in english and mandarin. In: International conference on machine learning. pp. 173–182. PMLR (2016)
2. An, W., Yu, S., Makihara, Y., Wu, X., Xu, C., Yu, Y., Liao, R., Yagi, Y.: Performance evaluation of model-based gait on multi-view very large population database with pose sequences. *IEEE Transactions on Biometrics, Behavior, and Identity Science* **2**(4), 421–430 (2020)
3. Bojarski, M., Del Testa, D., Dworakowski, D., Firner, B., Flepp, B., Goyal, P., Jackel, L.D., Monfort, M., Muller, U., Zhang, J., et al.: End to end learning for self-driving cars. *arXiv preprint arXiv:1604.07316* (2016)
4. Chao, H., He, Y., Zhang, J., Feng, J.: Gaitset: Regarding gait as a set for cross-view gait recognition. In: Proceedings of the AAAI conference on artificial intelligence. pp. 8126–8133 (2019)
5. Fan, C., Peng, Y., Cao, C., Liu, X., Hou, S., Chi, J., Huang, Y., Li, Q., He, Z.: Gaitpart: Temporal part-based model for gait recognition. In: Proceedings of the IEEE/CVF conference on computer vision and pattern recognition. pp. 14225–14233 (2020)
6. He, K., Gkioxari, G., Dollár, P., Girshick, R.: Mask r-cnn. In: Proceedings of the IEEE international conference on computer vision. pp. 2961–2969 (2017)
7. Hou, S., Cao, C., Liu, X., Huang, Y.: Gait lateral network: Learning discriminative and compact representations for gait recognition. In: European Conference on Computer Vision. pp. 382–398. Springer (2020)
8. Huang, H., Yang, W., Chen, X., Zhao, X., Huang, K., Lin, J., Huang, G., Du, D.: Eanet: Enhancing alignment for cross-domain person re-identification. *arXiv preprint arXiv:1812.11369* (2018)
9. Iwama, H., Okumura, M., Makihara, Y., Yagi, Y.: The ou-isir gait database comprising the large population dataset and performance evaluation of gait recognition. *IEEE Transactions on Information Forensics and Security* **7**(5), 1511–1521 (2012)
10. Jadon, S.: A survey of loss functions for semantic segmentation. In: 2020 IEEE Conference on Computational Intelligence in Bioinformatics and Computational Biology (CIBCB). pp. 1–7. IEEE (2020)
11. Kanazawa, A., Black, M.J., Jacobs, D.W., Malik, J.: End-to-end recovery of human shape and pose. In: Proceedings of the IEEE conference on computer vision and pattern recognition. pp. 7122–7131 (2018)
12. Kato, H., Ushiku, Y., Harada, T.: Neural 3d mesh renderer. In: Proceedings of the IEEE conference on computer vision and pattern recognition. pp. 3907–3916 (2018)
13. LeCun, Y., Bengio, Y., Hinton, G.: Deep learning. *nature* **521**(7553), 436–444 (2015)
14. Li, X., Makihara, Y., Xu, C., Yagi, Y., Yu, S., Ren, M.: End-to-end model-based gait recognition. In: Proceedings of the Asian conference on computer vision (2020)
15. Liao, R., Yu, S., An, W., Huang, Y.: A model-based gait recognition method with body pose and human prior knowledge. *Pattern Recognition* **98**, 107069 (2020)
16. Lin, B., Zhang, S., Yu, X.: Gait recognition via effective global-local feature representation and local temporal aggregation. In: Proceedings of the IEEE/CVF International Conference on Computer Vision. pp. 14648–14656 (2021)

17. Loper, M., Mahmood, N., Romero, J., Pons-Moll, G., Black, M.J.: Smpl: A skinned multi-person linear model. *ACM transactions on graphics (TOG)* **34**(6), 1–16 (2015)
18. Ronneberger, O., Fischer, P., Brox, T.: U-net: Convolutional networks for biomedical image segmentation. In: International Conference on Medical image computing and computer-assisted intervention. pp. 234–241. Springer (2015)
19. Ruder, S.: An overview of gradient descent optimization algorithms. arXiv preprint arXiv:1609.04747 (2016)
20. Song, C., Huang, Y., Huang, Y., Jia, N., Wang, L.: Gaitnet: An end-to-end network for gait based human identification. *Pattern recognition* **96**, 106988 (2019)
21. Takemura, N., Makihara, Y., Muramatsu, D., Echigo, T., Yagi, Y.: Multi-view large population gait dataset and its performance evaluation for cross-view gait recognition. *IPSJ Transactions on Computer Vision and Applications* **10**(1), 1–14 (2018)
22. Teepe, T., Khan, A., Gilg, J., Herzog, F., Hörmann, S., Rigoll, G.: Gaitgraph: graph convolutional network for skeleton-based gait recognition. In: 2021 IEEE International Conference on Image Processing (ICIP). pp. 2314–2318. IEEE (2021)
23. Winter, D.A.: Biomechanics and motor control of human gait: normal, elderly and pathological (1991)
24. Wu, Z., Huang, Y., Wang, L., Wang, X., Tan, T.: A comprehensive study on cross-view gait based human identification with deep cnns. *IEEE transactions on pattern analysis and machine intelligence* **39**(2), 209–226 (2016)
25. Yu, S., Tan, D., Tan, T.: A framework for evaluating the effect of view angle, clothing and carrying condition on gait recognition. In: 18th International Conference on Pattern Recognition (ICPR’06). vol. 4, pp. 441–444. IEEE (2006)
26. Zhang, Y., Sun, P., Jiang, Y., Yu, D., Yuan, Z., Luo, P., Liu, W., Wang, X.: Bytetrack: Multi-object tracking by associating every detection box. arXiv preprint arXiv:2110.06864 (2021)
27. Zhang, Y., Huang, Y., Yu, S., Wang, L.: Cross-view gait recognition by discriminative feature learning. *IEEE Transactions on Image Processing* **29**, 1001–1015 (2019)
28. Zhang, Z., Tran, L., Liu, F., Liu, X.: On learning disentangled representations for gait recognition. *IEEE Transactions on Pattern Analysis and Machine Intelligence* (2020)
29. Zhang, Z., Tran, L., Yin, X., Atoum, Y., Liu, X., Wan, J., Wang, N.: Gait recognition via disentangled representation learning. In: Proceedings of the IEEE/CVF Conference on Computer Vision and Pattern Recognition. pp. 4710–4719 (2019)
30. Zheng, L., Yang, Y., Hauptmann, A.G.: Person re-identification: Past, present and future. arXiv preprint arXiv:1610.02984 (2016)
31. Zhu, Z., Guo, X., Yang, T., Huang, J., Deng, J., Huang, G., Du, D., Lu, J., Zhou, J.: Gait recognition in the wild: A benchmark. In: Proceedings of the IEEE/CVF International Conference on Computer Vision. pp. 14789–14799 (2021)